MOLECULAR IMAGING AND BIOLOGY

Mol Imaging Biol (2015) 17:140–148
DOI: 10.1007/s11307-014-0776-6

Published Online: 31 July 2014

World Molecular Imaging Society

RESEARCH ARTICLE

Application of Partial Volume Effect Correction and 4D PET in the Quantification of FDG Avid Lung Lesions

Ali Salavati,[1] Samuel Borofsky,[1] Teo K. Boon-Keng,[2] Sina Houshmand,[1] Benjapa Khiewvan,[1] Babak Saboury,[1] Ion Codreanu,[1] Drew A. Torigian,[1] Habib Zaidi,[3,4,5] Abass Alavi[1]

[1]*Department of Radiology, Hospital of the University of Pennsylvania, 3400 Spruce Street, Philadelphia, PA, USA*
[2]*Department of Radiation Oncology, Hospital of the University of Pennsylvania, Philadelphia, PA, USA*
[3]*Division of Nuclear Medicine and Molecular Imaging, Geneva University Hospital, CH-1211, Geneva, Switzerland*
[4]*Geneva Neuroscience Center, Geneva University, CH-1211, Geneva, Switzerland*
[5]*Department of Nuclear Medicine and Molecular Imaging, University Medical Center Groningen, University of Groningen, 9700 RB, Groningen, The Netherlands*

Abstract

Purpose: The aim of this study is to assess a software-based method with semiautomated correction for partial volume effect (PVE) to quantify the metabolic activity of pulmonary malignancies in patients who underwent non-gated and respiratory-gated 2-deoxy-2-[^{18}F]fluoro-D-glucose (FDG)-positron emission tomography (PET)/x-ray computed tomography(CT).

Procedures: The study included 106 lesions of 55 lung cancer patients who underwent respiratory-gated FDG-PET/CT for radiation therapy treatment planning. Volumetric PET/CT parameters were determined by using 4D PET/CT and non-gated PET/CT images. We used a semiautomated program employing an adaptive contrast-oriented thresholding algorithm for lesion delineation as well as a lesion-based partial volume effect correction algorithm. We compared respiratory-gated parameters with non-gated parameters by using pairwise comparison and interclass correlation coefficient assessment. In a multivariable regression analysis, we also examined factors, which can affect quantification accuracy, including the size of lesion and the location of tumor.

Results: This study showed that quantification of volumetric parameters of 4D PET/CT images using an adaptive contrast-oriented thresholding algorithm and 3D lesion-based partial volume correction is feasible. We observed slight increase in FDG uptake by using PET/CT volumetric parameters in comparison of highest respiratory-gated values with non-gated values. After correction for partial volume effect, the mean standardized uptake value (SUVmean) and total lesion glycolysis (TLG) increased substantially (p value <0.001). However, we did not observe a clinically significant difference between partial volume corrected parameters of respiratory-gated and non-gated PET/CT scans. Regression analysis showed that tumor volume was the main predictor of quantification inaccuracy caused by partial volume effect.

Electronic supplementary material The online version of this article (doi:10.1007/s11307-014-0776-6) contains supplementary material, which is available to authorized users.

Correspondence to: Abass Alavi; *e-mail:* abass.alavi@uphs.upenn.edu

Conclusions: Based on this study, assessment of volumetric PET/CT parameters and partial volume effect correction for accurate quantification of lung malignant lesions by using respiratory non-gated PET images are feasible and it is comparable to gated measurements. Partial volume correction increased both the respiratory-gated and non-gated values significantly and appears to be the dominant source of quantification error of lung lesions.

Key words: FDG-PET/CT, Respiratory gating, Partial volume effect, Metabolic activity quantification, Lung cancer

Introduction

Integrated positron emission tomography/x-ray computed tomography (PET/CT) imaging is widely used for the diagnosis and staging of patients with various types of thoracic lesions [1–3]. However, PET data acquisition occurs over many respiratory cycles and as such, accurate evaluation of thoracic lesions on PET/CT may prove challenging due to respiratory motion during imaging. This may result in a blurring artifact, affecting standardized uptake value (SUV) quantification and volume measurement of lesions [4].

Various methods such as shallow breathing, breath-holding, and respiration synchronized techniques have been employed to reduce respiratory motion artifacts during PET acquisition [5–7]. One of the most commonly used techniques is respiratory gating, which consists in dividing a PET dataset into distinct phases of the respiratory cycle [8, 9]. Respiratory cycle information may be obtained with the use of external devices (pressure sensor belts or spirometry systems) or by internal, data-driven methods [10, 11]. Each respiratory cycle is separated into various bins using this monitoring information, and the corresponding PET data are binned and reconstructed into gated images [12]. 4D-CT and 4D-PET data are binned according to the gating scheme, which can be either phase- or amplitude-based. In phase-based respiratory gating, the respiratory cycle is divided into separate phase ranges, while amplitude gating divides the respiratory amplitude into different amplitude ranges [13]. In 2002, Nehmeh et al. were the first to perform respiratory gating for PET scanning in clinical setting and found that respiratory gating decreases total lesion volume and increases measured SUV compared to non-gated images [14]. Gating has also been reported to improve the diagnosis of malignant lung lesions and the evaluation of response to radiation treatment [15–18].

In addition to respiratory motion, partial volume effect which arises from the finite spatial resolution of the scanner also results in inaccurate PET image quantification, particularly when the tumor size is less than two to three times the scanner's spatial resolution [19–21]. While gating may reduce motion artifacts, it fails to correct the partial volume effect (PVE) and PVE is most likely to dominate over motion effects for small lesions [16]. Some approaches have been suggested for PVE correction or combined motion and PVE correction [17, 22]. However, it remains unclear how 4D PET/CT results are impacted by partial volume correction of metabolic lung lesions in the clinical setting.

In this study, we aim to employ a combined adaptive contrast-oriented thresholding segmentation and local background partial volume correction algorithm to calculate and compare the partial volume-corrected quantitative 2-deoxy-2-[^{18}F]fluoro-D-glucose (FDG) uptake parameters of lung lesions acquired using non-gated and 4D FDG PET/CT studies.

Materials and Methods

Study Population

The study population included consecutive 55 subjects (32 women and 23 men, mean age 66.5±9.5 years) with FDG avid lung lesions who underwent FDG-PET/CT radiation treatment simulation. The imaging protocol included both static and 4D PET scans in a single session. Surgical pathology reports were reviewed to confirm malignancy and tumor histology. This retrospective study was conducted following approval from the institutional review board at the Hospital of the University of Pennsylvania along with a Health Insurance Portability and Accountability Act (HIPAA) waiver.

Whole Body PET/CT Image Acquisition

All FDG-PET/CT scans were acquired using a whole-body PET/CT scanner with time-of-flight capability (Gemini TF Big Bore, Philips Healthcare, Bothell, WA). All patients fasted for at least 6 h and serum glucose levels were verified to be <200 mg/dl before intravenous injection of 444–555 MBq (12–15 mCi) of FDG. As part of the imaging protocol, static whole body PET images were acquired from the base of the skull to the mid thighs approximately 60 min after FDG administration for 3 min per bed position for diagnostic purposes. Image reconstruction was performed using LOR-TF-RAMLA ("BLOB-OS-TF") with 33 ordered subsets and 3 iterations. The manufacturer's software included normalization, attenuation, randoms, and scatter corrections. Energy rescaled low-dose CT images were used for attenuation correction of PET images. Non-gated and gated PET and CT images were reconstructed at 4 and 3 mm nominal slice thicknesses, respectively.

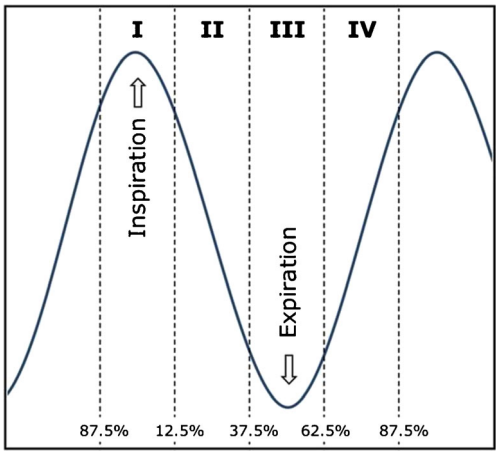

Fig. 1 Schematic representation of the respiratory cycle divided into four respiratory gates.

Respiratory-Gated PET/CT Image Acquisition of Lungs

Immediately after the static PET scan, a respiratory-gated 4D PET scan of the whole lung was performed with the patient in the same position by use of the real-time position management (RPM) respiratory gating system (Varian Medical Systems Inc., Palo Alto, CA). This gating system utilizes external infrared markers that are placed on a block that sits on the patient's chest. Respiration causes movement of these markers, which is then detected by a camera with an infrared illuminator. A computer stores data in the form of time and displacement of the infrared markers. The respiratory signal is used to sort the list mode data into four phase bins from which four PET images, each corresponding to a phase in the respiratory cycle, are reconstructed. The phase bins correspond to data obtained from 87.5 to 12.5 % (bin 1), 12.5 to 37.5 % (bin 2), 37.5 to 62.5 % (bin 3), and 62.5 to 87.5 % (bin 4) of one full respiratory cycle (Fig. 1). The 4D PET/CT scan included the thoracic region only and consisted of a 4D CT followed by 4D PET for 6 min per bed position. The phase-matched CT was also used for attenuation correction of PET images. The effectiveness of respiratory gating was evaluated by the assessment of plots displaying the frequency of PET data being placed into the four bins. Examples of such plots obtained in patients with regular and irregular breathing are shown (Fig. 2). In addition to the gated PET images, a static non-gated PET was reconstructed from the same raw data and used in the comparison between the gated and non-gated PET images.

Image Analysis

We measured metabolically active tumor volumes (MTV), SUVmax, SUVmean, total lesion glycolysis (TLG=SUVmean*MTV), partial volume corrected SUVmean (pvcSUVmean), partial volume corrected total lesion glycolysis (TLG=SUVmean*MTV), and SUVpeak of FDG avid thoracic lesions on both non-gated and respiratory-gated PET images (Fig. 3). To accomplish this, we employed an adaptive contrast-oriented thresholding algorithm, which permits delineation of the boundaries of lesions based on PET images alone. This modified adaptive thresholding delineation technique combines automatically determined background correction and local adaptive thresholding in an iterative model (ROVER software, ABX, Radeberg, Germany). The method used for partial volume correction (PVC) is described in detail in [18]. In brief, the algorithm takes as input the region of interest (ROI) boundaries and the estimated spatial resolution (full width at half maximum; FWHM) of the image data. A spillout region is defined as a concentric shell with a distance of 1×FWHM to the ROI boundaries and a background region is defined as shell with a distance of 1.5×FWHM to the spillout region. For each voxel inside the spillout region, the local background is subtracted. In this way, the effective spillout (spillout from ROI minus spillin from background) is computed and the resulting activity concentration is added to the mean value of the ROI. Hofheinz and colleagues [18] showed that the algorithm is not sensitive to the estimated FWHM as long as the FWHM is not underestimated. Therefore, in our investigation, we used a rather conservative FWHM of 8 mm. The software also calculated SUVpeak by measuring FDG uptake of a spherical region of 1.2-cm diameter (1 cm^3) centered at the

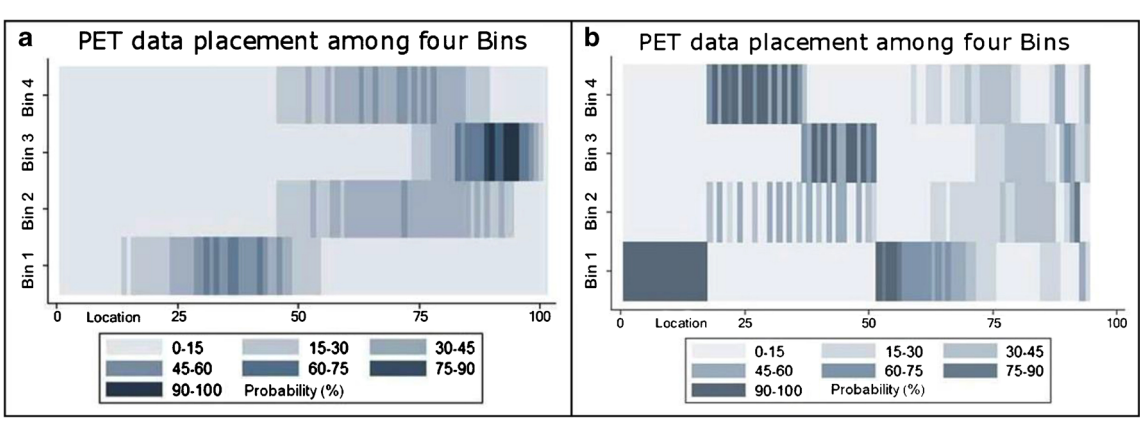

Fig. 2 **a** The effectiveness of respiratory gating was examined by constructing probability graphs that examined the frequency of PET data being placed into the four bins. The *x*-axis, location, refers to the displacement of a block placed on the patient's chest, which moves up and down with inspiration, thus providing the signal for respiratory waveforms. This graph shows an example of expected regular binning among four separate bins in a patient with regular breathing patterns. **b** Example of the ineffectiveness of phase-based binning in a patient with irregular respirations.

most active portion of the tumor. The accuracy and reproducibility of this methodology have previously been showed in previous studies [18, 23–26]. In this study, we also aimed to study inter-rater agreement of these algorithms in the assessment of 4D PET/CT. Therefore, one investigator described and specified slice number of each lesion in the PET/CT and then two other investigators quantified all lesions separately.

Considering that SUVs for small structures are more likely to be affected by the partial volume effect, lesions were subsequently divided into small (≤3 cm^3) and large (>3 cm^3) based on the MTV determined on initial non-gated PET images. The 3-cm^3 volume has been chosen arbitrarily to separate small lung lesions from large lung lesions based on previously used measurements reported in the literature [27–29].

Statistical Analysis

Continuous variables were expressed as mean±standard error of the mean (SEM) and tested for distribution normality. Bland-Altman [30], concordance correlation coefficient [31, 32], and coefficient of variation of duplicate measurements were used to assess agreement between the two raters' measurements. Interclass correlation coefficient and one-way analysis of variance (ANOVA) as well as post hoc Tukey-Kramer for pairwise comparisons were performed to assess any significant differences between non-gated and each of the four bins of respiratory-gated images. In addition to ANOVA, a paired *t* test between the highest gated SUVs and non-gated SUVs was performed. A two-sided *p* value of less than 0.05 was considered as significant. Since the accuracy of the respiratory gating and partial volume effect correction algorithms could be affected by the position of the tumor, we performed a subgroup analysis after classification of lesions according to their anatomical properties (upper lung, mediastinal, and lower lung) and lesion size (MTV<3 cm^3 or >3 cm^3). We assessed the partial volume effect by calculating the percentage of relative change of SUVmean [PVE= 100 * (pvcSUVmean-SUVmean)/SUVmean] for all lesions. In a multivariable regression analysis, we examined factors which can affect PVE, i.e., the size of lesion and the location of tumor. All data were analyzed using Stata software (Stata/IC Version 13.1, StataCorp, College Station, TX) and MedCalc (Version 13).

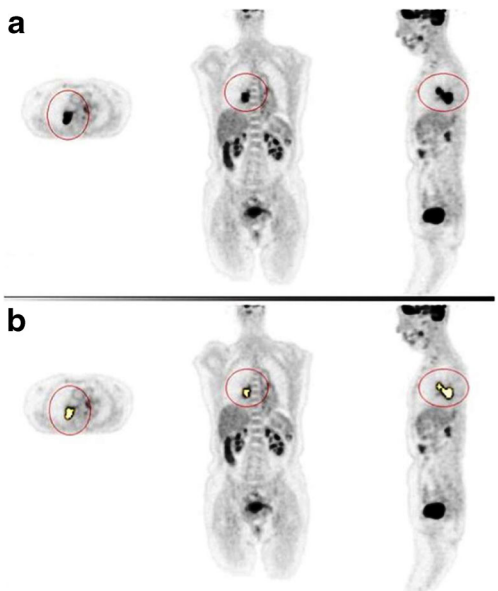

Fig. 3 **a** Axial, coronal, and sagittal PET images prior to ROI delineation but following mask placement about an FDG avid lesion. **b** Same images after ROI delineation by software method (b).

Table 1. Description of study cohort based on type of malignant lung lesion and disease stage

Type of malignant lung lesion or disease stage	Number
Squamous cell carcinoma	20
Adenocarcinoma	17
Small cell carcinoma	8
Extrathoracic pulmonary metastasis/poorly differentiated carcinoma	10
Stage I–II disease	12
Stage III disease	24
Stage IV disease	19

Results

Surgical pathology reports confirmed the presence of pulmonary malignancy in all 55 subjects included in the study. A summary of the types of malignancy and disease staging is provided in Table 1. A total of 106 lung lesions were identified, of which 76 had an MTV of greater than 3 cm^3 and 30 less than or equal to 3 cm^3; and 26 lesions were in upper lung, 49 lesions were mediastinal/middle lung, and 31 lesions were in the lower lung. Interpreter agreements were almost perfect for all parameters with concordance correlation coefficient ranging from 0.993 to 0.999 and coefficient of variation of duplicate measurements less than ten for all indices (Table 2) (Supplementary Figs. 1–4).

Gated Versus Non-Gated

Bland-Altman agreement analysis showed a good agreement between the highest gated phase and non-gated SUVs (Fig. 4). However, comparison of values of each bin and non-gated values did not show any statistically significant difference (Table 3). Pairwise comparison showed slight increase in the highest gated SUVs over

Table 2. This semiautomatic method of quantification shows substantial inter-rater agreement

	Concordance correlation coefficient (CCC) (95 % CI)	Coefficient of variation (%) of duplicate measurements
SUVmax	0.998 (0.997–0.999)	2.5
SUVmean	0.998 (0.997–0.999)	3.5
TLG	0.998 (0.997–0.998)	6.5
pvcSUVmean	0.993 (0.991–0.994)	4.1
MTV	0.996 (0.995–0.997)	8.9
pvcTLG	0.998 (0.998–0.999)	5.7

Two raters measured all PET scans separately. In sum, 520 measurements were compared

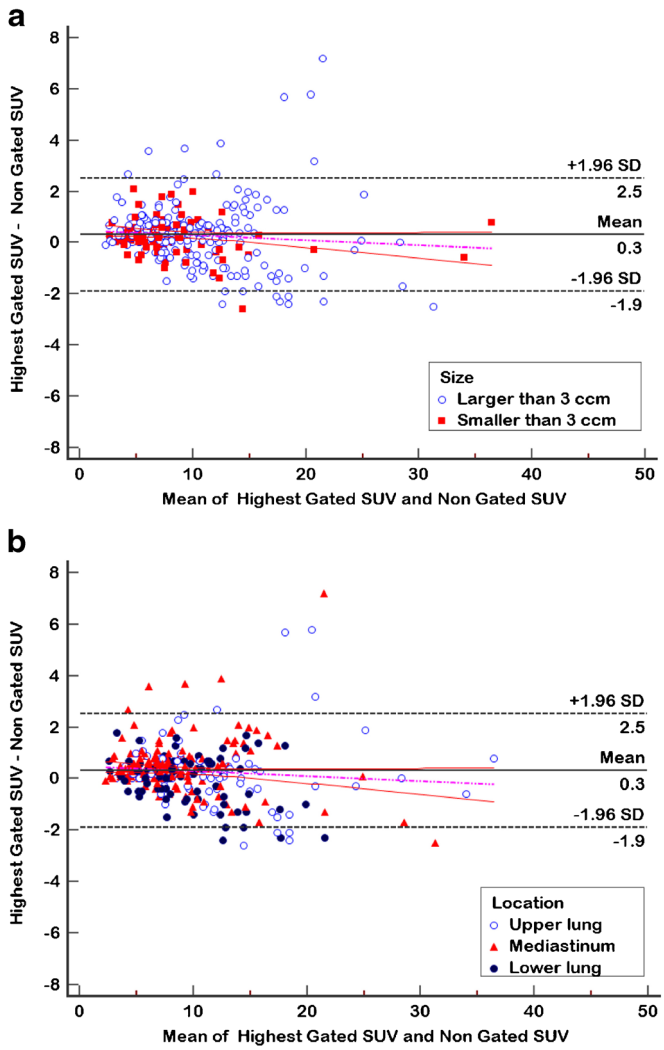

Fig. 4 Bland-Altman agreement plot for the variables obtained from highest respiratory-gated SUVs versus non-gated SUVs. The main cluster of points is well defined and located around the 0 line with relatively symmetric distribution on both sides. The *pink dash-dot line* is regression line of difference and *orange lines* are 95 % CI of regression line. The agreement analysis showed substantial concordance correlation coefficients for both SUV and MTV values (Tables 3 and 5).

non-gated SUVs (Table 4). Similarly, comparison of values of each bin and non-gated values did not show any statistically significant difference among lesions with MTV less than or equal to 3 cm^3 (Table 5). Pairwise comparison showed slight increase in highest gated pvcSUVmean over non-gated pvcSUVmean (Table 4).

Partial Volume Correction

Correction for partial volume effect increases the SUVmean significantly (55 % relative increase, p value <0.001). In subgroup analysis, the difference between PVE of lesions with MTV less than 3 cm^3 (74 % relative increase) and

Table 3. Metabolically active volume (MTV) and standardized uptake values (SUVs) in different phases of respiratory-gated PET/CT (>3 cm^3 lesions)

	Gated phase I	Gated phase II	Gated phase III	Gated phase IV	Non-gated	Intraclass correlation coefficient (95 % CI)	ANOVA (p value)
Lesion SUV_{max}	11.3±0.6	11.6±0.6	11.5±0.6	11.2±0.7	11.7±0.6	0.995 (0.993–0.997)	0.96
Lesion SUV_{mean}	7.0±0.3	7.1±0.3	7.1±0.3	6.8±0.4	7.1±0.4	0.996 (0.994–0.997)	0.95
Lesion $pvcSUV_{mean}$	10.2±0.5	10.7±0.6	10.5±0.6	10.1±0.6	10.6±0.6	0.992 (0.989–0.994)	0.96
Lesion SUV_{peak}	8.0±0.4	8.1±0.3	8.1±0.4	7.8±0.4	8.3±0.5	0.995 (0.993–0.997)	0.84
MTV (cm^3)	25.8±3.4	25.4±3.5	26.2±3.6	27.9±4.0	26.4±3.6	0.998 (0.997–0.998)	0.98

All data are presented as mean±SEM

Table 4. Pairwise comparison between highest respiratory-gated SUVs and non-gated SUVs

	Total	*P* value	Smaller than 3 cm^3	*P* value	Larger than 3 cm^3	*P* value	Upper lung+ mediastinal	*P* value	Lower lung	*P* value
Number of lesions	106		30		76		75 (26+49)		31	
SUVmax of non-respiratory-gated	10.8±0.5	0.009	8.3±1.1	0.07	11.7±0.6	0.03	10.1±0.5	0.1	12.6±1.5	0.1
Highest SUVmax of respiratory-gated	11.2±0.5	8.6±1.0	12.1±0.6	10.3±0.5	13.1±1.4					
SUVmean of non-respiratory-gated	6.6±0.3	0.1	5.4±0.6	0.26	7.1±0.4	0.17	6.3±0.3	0.3	7.6±0.8	0.2
Highest SUVmean of respiratory-gated	6.8±0.3	5.5±0.6	7.3±0.3	6.4±0.3	7.9±0.8					
pvcSUVmean of non-respiratory-gated	10.4±0.5	0.001	9.7±1.0	0.04	10.6±0.6	0.002	9.6±0.5	0.002	12.1±1.4	0.04
Highest pvcSUVmean of respiratory-gated	10.9±0.6	10.1±1.0	11.2±0.5	10.1±0.4	13.1±1.4					
SUVpeak of non-respiratory-gated	7.3±0.4	0.7	4.7±0.7	0.9	8.3±0.4	0.7	6.8±0.3	0.2	8.5±1.1	0.5
Highest SUVpeak of respiratory-gated	7.4±0.4	4.8±0.6	8.3±0.4	6.9±0.4	8.4±0.9					

higher than 3 cm^3 (48 % relative increase) was statistically significant (p value <0.0001). In the regression model, the size of lesion was the only statistically significant predictor of PVE (percentage of relative increase of SUVmean following partial volume correction) while the R^2 of 0.451, p value <0.0001, slope of −24.69 (95 % CI −29.96, −19.35), and Pearson r correlation coefficient=−0.67 (95 % CI −0.76, −0.55) (Fig. 5).

Discussion

This study showed that quantification of volumetric parameters of 4D PET/CT images using an adaptive contrast-oriented thresholding algorithm and 3D lesion-based partial volume correction is feasible, and we observed only a slight increase in the quantification of metabolic activity of lung malignancies using the highest respiratory-gated versus non-gated PET/CT images which is in contrast to previous respiratory-gated PET/CT studies [14, 33]. Partial volume correction increased both the respiratory-gated and non-gated values significantly and appears to be the dominant source of quantitative error of lung malignancies.

Motion effects during PET acquisition causes image blurring and results in activity spillover into surrounding background. This PET-based approach for partial volume correction seeks to recover the spillover activity in the computation of SUV. It is for this reason that partial volume correction methods can be used to recover the decrease in SUV in non-gated PET images which is affected by motion blurring. Of note is that this method appeared successful even for small lesions with a MTV less than or equal to 3 cm^3. The reason why a PVE correction approach is effective for both large and small lesions can be explained qualitatively by considering the relative detrimental effects of PVE and smearing due to motion. For large lesions, motion has a small impact on SUV calculations [16]. For small lesions, PVE dominates over motion blurring and thus using a PVE approach by treating motion as a small addition to PVE blurring results in corrected SUV of gated PET to be close in value to those from a non-gated PET.

While respiratory gating has been shown to be effective in reducing motion artifacts and minimizing the field of radiation treatment for lung lesions, it is not completely devoid of limitations. 4D PET/CT reduces motion artifacts at the cost of decreasing signal-to-noise ratio (SNR), since during PET acquisition, non-gated images use all detected counts, while each of the phase gating bins contains only a fraction of the total counts [7]. To achieve similar image SNR as that of the non-gated image, one can increase the acquisition time, which is not desirable in the current clinical practice [7, 34], and this commonly results in increased radiation exposure from CT imaging [35], particularly for gated PET/CT protocols that utilize a phase-correlated 4D CT for attenuation correction. Another option is to use direct 4D reconstruction with an organ motion model

Table 5. Metabolically active volume (MTV) and standardized uptake values (SUVs) in different phases of respiratory gated PET/CT (≤3 cm^3 lesions)

	Gated phase I	Gated phase II	Gated phase III	Gated phase IV	Non-gated	Intraclass correlation coefficient (95 % CI)	ANOVA (*p* value)
Lesion SUV_{max}	8.3±0.9	8.2±0.8	8.4±0.8	8.0±0.9	8.5±1.0	0.997 (0.995–0.998)	0.97
Lesion SUV_{mean}	5.3±0.27	5.2±0.26	5.4±0.29	5.2±0.26	5.5±0.34	0.997 (0.995–0.998)	0.96
Lesion $pvcSUV_{mean}$	9.3±0.9	8.9±0.8	9.5±0.8	9.2±0.9	9.8±1.0	0.992 (0.990–0.994)	0.94
Lesion SUV_{peak}	4.6±0.6	4.6±0.6	4.7±0.6	4.5±0.6	4.8±0.7	0.998 (0.996–0.999)	0.98
MTV (cm^3)	1.8±0.1	1.9±0.2	1.7±0.2	1.7±0.1	1.7±0.1	0.967 (0.944–0.982)	0.97

All data are presented as mean±SEM

enabling to account for all information acquired to reduce the noise [8, 9].

In addition, breathing irregularities can significantly reduce the quantification accuracy of 4D PET images and results in FDG uptake values that lie between the true (stationary) and non-gated values [13, 16, 36]. Typical respiratory patterns commonly demonstrate irregularities rather than a smooth, sinusoidal curve, and such patterns were encountered in our study in some subjects (Fig. 3) [36]. Ideally, phase-based gating will place large respiratory amplitude data into inspiratory phases and small amplitude data into expiratory phases. However, typical breathing irregularities, such as a short deep inspiratory phase, frequently results in erroneous placement of large and small amplitude data into wrong bins [13]. Large breaths may also lead to desynchronization of PET and CT, which can affect coregistration and translate into diagnostic errors [37]. The technique also requires patient compliance, and often additional therapist participation. However, it may not be well-tolerated by patients with compromised lung function, such as in many lung cancer patients.

Our results suggest that PVE represent the dominant source of quantification error and breathing motion causes smaller degree of inaccuracy. In addition, gated acquisition is cumbersome and not optimum in patients with irregular respiratory patterns, while PVE correction can be performed automatically after image acquisition.

Our study has some limitations. First, this study evaluated differences in PET indices obtained by respiratory-gated and non-gated images, which may be relevant for evaluation of interval changes in tumor metabolic activity. However, it should be noted that tumor size determined with PVE correction software is a metabolic size, which may not always correspond to the CT- or MRI-based morphological size or provide sufficient information related to lesional anatomy and its range of motion during a respiratory cycle. Since the morphological parameters may prove essential during radiation therapy, our results should not be extended to PET/CT studies performed for radiation treatment planning where the accuracy of SUV quantification may be less important. Second, it has been demonstrated that phase-based respiratory gating is less effective than amplitude-based gating, especially in patients with irregular respiratory cycles [13]. Despite this knowledge, phase-based methods of gating remain the most widely investigated in cancer research [15], as in the current study. In addition, six

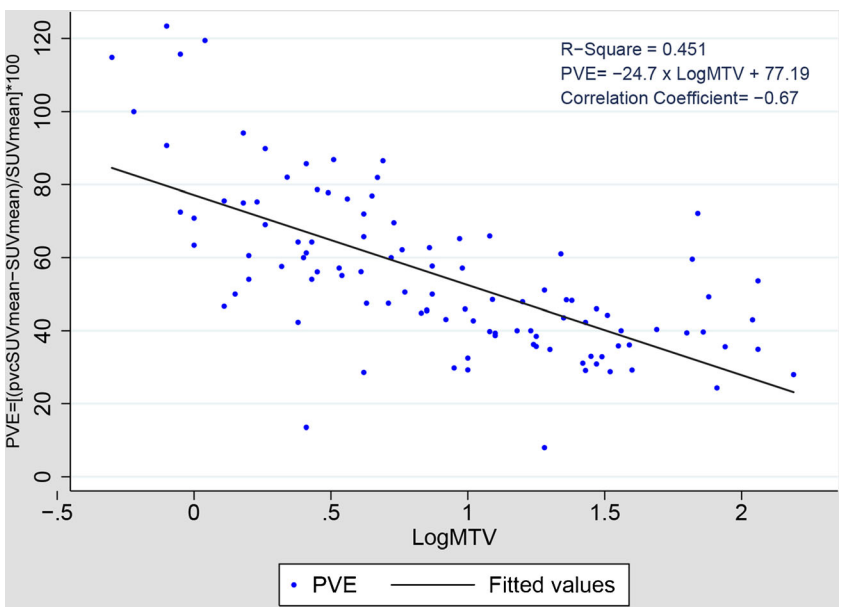

Fig. 5 In regression analysis, the only predictive factor of PVE [100*(pvcSUVmean-SUVmean)/SUVmean] was lesion volume. We use log-transformed MTV in our regression model since it shows more symmetric distribution than non-transformed MTV. R^2=0.451, *p* value <0.0001, Pearson's *r* correlation coefficient=−0.67 (95 % CI −0.76 to −0.55).

respiratory gates have been suggested as the optimal number in phase-based respiratory gating [38], while we used only four phase gates in order to limit image noise. Third, histopathological measurement of the actual volume of lung lesions was not performed as the reference standard for assessment of lesion volume, although this is also prone to errors related to processing of *ex vivo* specimens and inclusion of nonlesional tissues as part of volumetric measurement of the lesion. Fourth, given the retrospective nature of the study, we were unable to coach subjects or to correct for detected irregular breathing. However, some studies have shown that patients can be coached to assist in regular breathing parents, others have found that coaching increases patient anxiety [39, 40] and that about half of the patients could not follow both audio and video instructions simultaneously [41]. Fifth, in addition to analyzing the whole population of tumors, subgroup analyses also did not show any significant differences between gated and non-gated parameters. Further studies with larger sample size are warranted to validate these findings. Sixth, we used a semiautomatic PVE correction algorithm, which is feasible for solitary lesions; however, it is time-consuming for cases with multiple lesions [25, 42]. We believe there is a dire need for robust automatic operator-friendly quantification software with PVE correction capabilities—an omission which will hopefully be addressed by manufacturers in the near future [42]. Considering the large number of reported PET image segmentation and partial volume correction strategies, the lack of a standardized benchmark for evaluation and validation, and since most of the published techniques are not currently implemented in commercial software, recommending a specific algorithm is challenging and premature. However, the most promising techniques for PET image segmentation are those based on the use of active contours taking advantage of multimodality imaging and stochastic modeling, whereas multiresolution and structural-functional synergistic resolution recovery approaches seem have many attractive features for partial volume correction. However, as different PVE algorithms may be optimal for different sites, e.g., brain versus lung, it becomes challenging for manufacturers to implement a PVE correction method that will perform well for all sites. Seventh, delineation and partial volume effect correction methods used in this study, as well as other available quantification methods, have some limitations and it could affect the results of this study in particular for small lesions. The algorithms used by ROVER were mainly validated using phantom studies. However, the accuracy reached in phantom studies is unlikely to be reached in clinical setting. It should be emphasized that none of the algorithms proposed so far is characterized or understood enough to enable its use in clinical setting without a cautious knowledgeable check [43].

The comparison of manual measurements of non-gated and respiratory-gated PET/CT scans with those obtained by software-based methods with semiautomated correction for PVE, comparison of the potential advantages and disadvantages of different PVE correction algorithms, factors which affect different segmentation and PVE correction algorithms, tracer uptake heterogeneity, impact of lesion shape on PVE, and our PVE correction method and assessment of test-retest (repeatability) performance of measurements of the same patient within a short period are beyond the scope of this article and may represent a new topic for further research.

Conclusion

Our results suggest that assessment of volumetric PET/CT parameters and partial volume correction for quantification of lung malignant lesions by using respiratory non-gated PET images are feasible and comparable to gated measurements. Partial volume correction increased both the respiratory-gated and non-gated values significantly and appears to be a potential source of quantification error, particularly in small lesions. These preliminary results are promising; however, still likely require validation using further prospective larger-scale studies. Novel strategies aiming at applying direct 4D PET image reconstruction methods to motion compensation show potential but remain to be further improved and/or constrained to guarantee consequential reconstructions.

Acknowledgments. This work was supported by the Swiss National Science Foundation under grant SNSF 31003A-149957.

Conflict of Interest. The authors declare that they have no conflict of interest.

References

1. Gould MK, Kuschner WG, Rydzak CE et al (2003) Test performance of positron emission tomography and computed tomography for mediastinal staging in patients with non-small-cell lung cancer: a meta-analysis. Ann Intern Med 139:879–892
2. Paulino AC, Thorstad WL, Fox T (2003) Role of fusion in radiotherapy treatment planning. Semin Nucl Med 33:238–243
3. Salavati A, Basu S, Heidari P, Alavi A (2009) Impact of fluorodeoxyglucose PET on the management of esophageal cancer. Nucl Med Commun 30:95–116
4. Erdi YE, Nehmeh SA, Pan T et al (2004) The CT motion quantitation of lung lesions and its impact on PET-measured SUVs. J Nucl Med 45:1287–1292
5. Daouk J, Fin L, Bailly P, Meyer ME (2009) Respiratory-gated positron emission tomography and breath-hold computed tomography coupling to reduce the influence of respiratory motion: methodology and feasibility. Acta Radiol 50:144–155
6. Nehmeh SA, Erdi YE, Meirelles GS et al (2007) Deep-inspiration breath-hold PET/CT of the thorax. J Nucl Med 48:22–26
7. Liu C, Alessio A, Pierce L et al (2010) Quiescent period respiratory gating for PET/CT. Med Phys 37:5037–5043
8. Li T, Thorndyke B, Schreibmann E, Yang Y, Xing L (2006) Model-based image reconstruction for four-dimensional PET. Med Phys 33:1288–1298
9. Rahmim A, Tang J, Zaidi H (2009) Four-dimensional (4D) image reconstruction strategies in dynamic PET: beyond conventional independent frame reconstruction. Med Phys 36:3654–3670
10. Kesner AL, Kuntner C (2010) A new fast and fully automated software based algorithm for extracting respiratory signal from raw PET data and its comparison to other methods. Med Phys 37:5550–5559
11. Nehmeh SA, Erdi YE (2008) Respiratory motion in positron emission tomography/computed tomography: a review. Semin Nucl Med 38:167–176

12. He J, O'Keefe GJ, Jones G et al (2007) Evaluation of geometrical sensitivity for respiratory motion gating by GATE and NCAT simulation. Conf Proc IEEE Eng Med Biol Soc 2007:4165–4168
13. Dawood M, Lang N, Jiang X, Schafers KP (2006) Lung motion correction on respiratory gated 3-D PET/CT images. IEEE Trans Med Imaging 25:476–485
14. Nehmeh SA, Erdi YE, Ling CC et al (2002) Effect of respiratory gating on quantifying PET images of lung cancer. J Nucl Med 43:876–881
15. Chang G, Chang T, Pan T, Clark JW Jr, Mawlawi OR (2010) Implementation of an automated respiratory amplitude gating technique for PET/CT: clinical evaluation. J Nucl Med 51:16–24
16. Teo BK, Saboury B, Munbodh R et al (2012) The effect of breathing irregularities on quantitative accuracy of respiratory gated PETCT. Med Phys 39:7390–7397
17. Basu S, Alavi A (2008) Feasibility of automated partial-volume correction of SUVs in current PET/CT scanners: can manufacturers provide integrated, ready-to-use software? J Nucl Med 49:1031–1032. doi:10.2967/jnumed.108.050401, author reply 1032–1033
18. Hofheinz F, Langner J, Petr J et al (2012) A method for model-free partial volume correction in oncological PET. EJNMMI Res 2:16
19. Soret M, Bacharach SL, Buvat I (2007) Partial-volume effect in PET tumor imaging. J Nucl Med 48:932–945
20. Basu S, Zaidi H, Houseni M et al (2007) Novel quantitative techniques for assessing regional and global function and structure based on modern imaging modalities: implications for normal variation, aging and diseased states. Semin Nucl Med 37:223–239
21. Rousset O, Rahmim A, Alavi A, Zaidi H (2007) Partial volume correction strategies in PET. PET Clin 2:235–249
22. Chang G, Chang T, Pan T, Clark JW Jr, Mawlawi OR (2010) Joint correction of respiratory motion artifact and partial volume effect in lung/thoracic PET/CT imaging. Med Phys 37:6221–6232
23. Torigian DA, Lopez RF, Alapati S et al (2011) Feasibility and performance of novel software to quantify metabolically active volumes and 3D partial volume corrected SUV and metabolic volumetric products of spinal bone marrow metastases on 18F-FDG-PET/CT. Hell J Nucl Med 14:8–14
24. Schaefer A, Kim YJ, Kremp S et al (2013) PET-based delineation of tumour volumes in lung cancer: comparison with pathological findings. Eur J Nucl Med Mol Imaging 40:1233–1244
25. Saboury B, Salavati A, Brothers A et al (2014) FDG PET/CT in Crohn's disease: correlation of quantitative FDG PET/CT parameters with clinical and endoscopic surrogate markers of disease activity. Eur J Nucl Med Mol Imaging 41:605–614
26. Abdulla S, Salavati A, Saboury B, Basu S, Torigian DA, Alavi A (2014) Quantitative assessment of global lung inflammation following radiation therapy using FDG PET/CT: a pilot study. Eur J Nucl Med Mol Imaging 41:350–356
27. Hickeson M, Yun MJ, Matthies A et al (2002) Use of a corrected standardized uptake value based on the lesion size on CT permits accurate characterization of lung nodules on FDG-PET. Eur J Nucl Med Mol Imaging 29:1639–1647
28. Vanderhoek M, Perlman SB, Jeraj R (2012) Impact of the definition of peak standardized uptake value on quantification of treatment response. J Nucl Med 53:4–11
29. Pepin A, Daouk J, Bailly P, Hapdey S, Meyer ME (2014) Management of respiratory motion in PET/computed tomography: the state of the art. Nucl Med Commun 35:113–122
30. Bland JM, Altman DG (1986) Statistical methods for assessing agreement between two methods of clinical measurement. Lancet 1:307–310
31. Lin LI (1989) A concordance correlation coefficient to evaluate reproducibility. Biometrics 45:255–268
32. Barnhart HX, Haber M, Song J (2002) Overall concordance correlation coefficient for evaluating agreement among multiple observers. Biometrics 58:1020–1027
33. Aristophanous M, Berbeco RI, Killoran JH et al (2012) Clinical utility of 4D FDG-PET/CT scans in radiation treatment planning. Int J Radiat Oncol Biol Phys 82:e99–105
34. Kawano T, Ohtake E, Inoue T (2008) Deep-inspiration breath-hold PET/CT of lung cancer: maximum standardized uptake value analysis of 108 patients. J Nucl Med 49:1223–1231
35. Daou D (2008) Respiratory motion handling is mandatory to accomplish the high-resolution PET destiny. Eur J Nucl Med Mol Imaging 35:1961–1970
36. Schafers KP, Stegger L (2008) Combined imaging of molecular function and morphology with PET/CT and SPECT/CT: image fusion and motion correction. Basic Res Cardiol 103:191–199
37. Nehmeh SA, Erdi YE, Pan T et al (2004) Four-dimensional (4D) PET/CT imaging of the thorax. Med Phys 31:3179–3186
38. Dawood M, Buther F, Stegger L et al (2009) Optimal number of respiratory gates in positron emission tomography: a cardiac patient study. Med Phys 36:1775–1784
39. Kini VR, Vedam SS, Keall PJ, Patil S, Chen C, Mohan R (2003) Patient training in respiratory-gated radiotherapy. Med Dosim 28:7–11
40. Lupi A, Zaroccolo M, Salgarello M, Malfatti V, Zanco P (2009) The effect of 18F-FDG-PET/CT respiratory gating on detected metabolic activity in lung lesions. Ann Nucl Med 23:191–196
41. Jiang SB (2006) Technical aspects of image-guided respiration-gated radiation therapy. Med Dosim 31:141–151
42. Salavati A, Saboury B, Alavi A (2014) Comment on: "tumor aggressiveness and patient outcome in cancer of the pancreas assessed by dynamic 18 F-FDG PET/CT". J Nucl Med 55:350–351
43. Zaidi H, El Naqa I (2010) PET-guided delineation of radiation therapy treatment volumes: a survey of image segmentation techniques. Eur J Nucl Med Mol Imaging 37:2165–2187